Blue-Shifting Hydrogen Bonds

Pavel Hobza*[,†,‡] and Zdeněk Havlas[‡,§]

J. Heyrovský Institute of Physical Chemistry, Academy of Sciences of the Czech Republic, 182 23 Prague 8, Czech Republic, Institute of Organic Chemistry and Biochemistry, Academy of Sciences of the Czech Republic, 166 10 Prague 6, Czech Republic, and Center for Complex Molecular Systems and Biomolecules, 182 23 Prague 8, Czech Republic

Received January 14, 2000

Contents

I. Introduction 4253
II. C–H···π Improper, Blue-Shifting H-Bond 4256
  1. Benzene···Carbon–Hydrogen-Donor Complexes 4256
  2. Fluorobenzene···HCX_3 (X = F, Cl) Complexes 4257
III. C–H···O Improper, Blue-Shifting H-Bond 4258
IV. C–H···F Improper, Blue-Shifting H-Bond 4260
V. C–H···X^- (X = Halogen) Improper, Blue-Shifting H-Bond 4260
VI. Nature of H-Bonding and Improper, Blue-Shifting H-Bonding 4261
  1. Role of Dispersion Energy 4261
  2. "Atoms in Molecules" (AIM) Topological Analysis 4261
  3. NBO Analysis of the Electronic Structure 4262
  4. Analysis of Molecular Orbitals 4263
VII. Conclusion 4263
VIII. Acknowledgments 4263
IX. References 4264

I. Introduction

Under certain conditions the interaction of atoms leads to formation of molecules. This type of interaction is relatively strong, with maximum of attraction between specific pairs of atoms (except in some special cases). These pairs of atoms form bonds. The bond character ranges from covalent to ionic over a spectrum of polar bonds. Weaker bonds which keep atoms, groups of atoms, or molecules together exist also. One of the strongest and most common is the hydrogen bond (H-bond). Although it is not easy to define H-bonds to include all the features ascribed to it by the different branches of science, these hydrogen bonds always describe an attractive interaction between two species (atoms, groups, molecules) in a structural arrangement where the hydrogen atom, which is covalently bound to one of the species, is placed in between of these species. An exception is the rare symmetrical ionic hydrogen bond.

* To whom correspondence should be addressed. Telephone: (+420) 2 6605 2056. Fax: (+420) 2 858 2307. E-mail: hobza@indy.jh-inst.cas.cz.
† J. Heyrovský Institute of Physical Chemistry, Academy of Sciences of the Czech Republic.
‡ Center for Complex Molecular Systems and Biomolecules.
§ Institute of Organic Chemistry and Biochemistry, Academy of Sciences of the Czech Republic.

The H-bond plays a key role in chemistry, physics, and biology, and its consequences, such as the properties of liquid and solid water, were observed before the bond was identified and named. For a historical survey, dating back to the beginning of 20th century, the reader is referred to first chapters of recently published monographs on H-bonding: *An Introduction to Hydrogen Bonding*[1] by Jeffrey, *The Weak Hydrogen Bond*[2] by Desiraju and Steiner, and *Hydrogen Bonding*[3] by Scheiner. The term "hydrogen bond" was probably used first by Linus Pauling in his paper[4] on the nature of chemical bond.

The importance of H-bonds is enormous. They are responsible[3] for the structure and properties of water, an essential compound for life, as a solvent and in its various phases. Further, H-bonds also play a key role in determining the shapes, properties, and functions of biomolecules.

The H-bond is a bond between electron-deficient hydrogen and a region of high electron density. Most frequently, a H-bond is of the X−H···Y type, where X and Y are electronegative elements and Y possesses one or more lone electron pairs. H-bonds having X,Y = F, O, and N are the most frequently and best studied.[1−3] For some time there were speculations whether an aromatic ring with its excess of electron density above and below the ring plane could also act as a hydrogen-bond acceptor.[2] Recently, the O−H···π H-bonds were detected for complexes of benzene with water and methanol[5,6] and similar complexes of fluorobenzene.[7,8] The concept of H-bonds was later extended to the C−H···Y bonding types. Examples where Y is an electronegative atom[9−11] or C−H···π types[6,8,12−16] have both been observed.

As mentioned above, the published definitions of the H-bond are not unambiguous and many exist.[17] The most recent definition of X−H···Y H-bonding originates from Popelier[18] and is based on topological properties of the electron density and a set of integrated atomic properties related to the hydrogen atom involved. The criteria for the existence of H-bonding are as follows: (i) correct topological pattern (i.e., the existence of a bond critical point (bcp) and a bond path); (ii) proper value of electron density and Laplacian of electron density at this bcp; (iii) penetration of H and Y atoms; (iv) increase of a hydrogen net charge; (v) energetic destabilization of hydrogen; (vi) decrease of dipolar polarization; (vii) decrease of hydrogen atomic volume. It is clear that this definition is cumbersome and too reliant on

10.1021/cr990050q CCC: $35.00
Published on Web 09/14/2000

Pavel Hobza was born in 1946 in Přerov, Czechoslovakia, and graduated from Czech Technical University in 1969. In 1974 he received his Ph.D. degree (with Professor R. Zahradník) and in 1988 his D.Sc. degree; after 1989 he became Associated Professor of Charles University in Prague. Since 1989 he has been employed at the J. Heyrovský Institute of Physical Chemistry, Czech Academy of Sciences, Prague. After postdoctoral study with Professor C. Sandorfy at the Université de Montréal, Montréal, he spent several periods as a visiting professor and a visiting scientist at Université de Montréal, Montréal, Friedrich-Alexander-Universität Erlangen-Nürnberg, and Technische Universität München. Since 1998 he has been Head of the Department of Chemical Physics at the J. Heyrovský Institute. He has been a fellow of the Learned Society of the Czech Republic since 1998. Dr. Hobza has authored or co-authored about 180 papers and two books. These studies dealt mainly with molecular interactions and their role in physical chemistry and biodisciplines.

Zdeněk Havlas was born in 1951 in Nymburk, Czech Republic, and graduated at the Charles University in 1975. In 1979 he received his Ph.D. degree at the Czechoslovak Academy of Sciences (with Dr. J. Beránek and Professor R. Zahradník). Since 1975 he has been employed at the Institute of Organic Chemistry and Biochemistry, Czech Academy of Sciences, Prague. After postdoctoral study with Professor W. Kolos at Warsaw University and Professor R. Hoffmann at Cornell University, Ithaca, NY, he spent two years at J. W. Goethe University, Frankfurt/Main, as a Humboldt stipendiant with Professor H. Bock. The cooperation with the Frankfurt University lasted for more than 10 years. In the last five years he has closely worked with Professor J. Michl, Colorado University at Boulder. Since 1998 he has been Head of the Department of Theoretical Chemistry at the Institute of Organic Chemistry and Biochemistry. Dr. Havlas has published over 110 papers and three books. His research interests cover applied quantum chemistry, structural chemistry, weak intermolecular interactions, chemical reactivity, and photochemistry.

calculated characteristics to be of practical use for experimentalists.

Two features are, however, common to all generally accepted variants of H-bonds. First, there is a significant charge transfer from the proton acceptor (Y) to the proton donor (X−H). Second, formation of the X−H···Y H-bond results in weakening of the X−H bond. This weakening is accompanied by bond elongation and a concomitant decrease of the X−H stretch vibration frequency compared to the noninteracting species. A shift to lower frequencies is called a red shift and represents the most important, easily detectable (in liquid, gas, and solid phases) manifestation of the formation of a H-bond. Note that these "significant" changes of molecular properties upon complex formation are actually quite small: the change in energies, bond lengths, frequencies, and electron densities are two or more orders of magnitude smaller than typical chemical changes. The red shift of the X−H stretch vibration, which varies between several tens or hundreds of wavenumbers, represented until recently unambiguous information about the formation of a H-bond, since the formation of a H-bond in a X−H···Y system is accompanied by weakening of the X−H covalent bond. This is the basis for several spectroscopic, structural, and thermodynamic techniques for the detection and investigation of H-bonding. The characteristic features[3] of X−H···Y H-bond are as follows: (i) the X−H covalent bond stretches in correlation with the strength of the H-bond; (ii) a small amount of electron density (0.01−0.03 e) is transferred from the proton-acceptor (Y) to the proton-donor molecule (X−H); (iii) the band which corresponds to the X−H stretch shifts to lower frequency (red shift), increases in intensity, and broadens. The value of the red shift and the strength of the H-bond are correlated.[3] Frequency shifts correlate with various characteristics of the H-bonded system. Recently relationschips were found between experimental proton affinities and frequency shifts as well as between ab initio-calculated bond distances, interaction energies, and frequency shifts (deduced from complexes of pyridines, pyrimidines, and imidazoles with water[19] and pyridine derivatives with water[20]).

The first indication that the situation is more complicated appeared in 1989 when Buděšínský, Fiedler, and Arnold reported the preparation and spectra of triformylmethane (TFM).[21] The authors measured the IR spectrum of TFM in chloroform and detected the presence of a distinct, sharp band close to the C−H stretch of chloroform but slightly shifted toward higher wavenumbers (3028 cm^{-1} compared to 3021 cm^{-1}, the typical C−H stretch value for chloroform). Therefore, instead of the normal red shift of the C−H stretch frequency, a blue shift was observed. The authors were certainly aware of the peculiarity of their finding: "We find it rather strange that this remarkable effect has not been observed by other authors[22] during their detailed examination of the IR spectrum of TFM".

The second observation of the blue shift was reported in 1997 by Boldeskul et al.[23] The authors measured the IR spectra of chloroform, deuterochloroform, and bromoform in mixed systems containing proton acceptors such as carboxy, nitro, and sulfo compounds. The formation of intermolecular complexes was accompanied by shifts of the haloform C−H/D stretch vibration absorption band by 3−8 cm^{-1} to higher frequency compared to their position in CCl_4. The unusual shift was explained by a

strengthening of the C−H/D bond due to increase of its s character caused by molecular deformation resulting from intermolecular forces. An attempt to explain[23] this unusual behavior of haloforms by semiempirical MNDO−H quantum chemical method failed. Contrary to experimental findings, calculations predicted a decrease of the C−H frequency (i.e., a red shift) upon formation of the intermolecular complexes. The authors of both papers (refs 21 and 23) promised to study the observed phenomenon (blue shift) further, but no other paper on this subject appeared.

The first systematic investigation of the blue shift of the X−H stretch frequency in X−H···Y complexes was a theoretical study of the interaction of benzene with C−H proton donors,[24] where it was shown that the formation of benzene···HCX (CX = CH_3, CCl_3, C_6H_5) complexes leads to a C−H bond contraction and an increase of the respective stretch frequency (blue shift). Because the most important feature (the shortening of the proton-donor C−H bond and the blue shift) were opposite to those characteristics of classical H-bonds (the elongation of the proton donor X−H bond and the red shift), we originally called this specific bonding type an "anti-hydrogen bond". The term anti-hydrogen bond was later rightfully criticized as misleading mainly because it could suggest a destabilizing interaction of the subsystems or suggest a complex with anti-hydrogen. The anti-H-bonded complexes are formally the same as the classical hydrogen bond: the proton is placed between both subsystems, charge is transferred from proton acceptor to proton donor system, and stabilization of the complex is comparable to a normal H-bond. The manifestation of both types of H-bond was, however, different. Because this characteristic feature is opposite and, moreover, since both types of H-bonds have different origins (see later), we prefer terms "H-bond" for the classical, red-shifting one and "improper, blue-shifting" for what was called an anti-H-bond.

The blue shift of the C−H stretch frequency of chloroform was first detected in solutions of TFM in chloroform[21] and nitrobenzene in chloroform.[23] Direct evidence of the blue shift in the gas phase was missing until 1999, when a complex between fluorobenzene and chloroform was investigated using the double-resonance infrared ion-depletion spectroscopy.[25] The experimental value of the blue shift of the chloroform C−H stretch frequency (14 cm^{-1}) agreed well with the theoretical prediction (12 cm^{-1}) using a good quality ab initio treatment (see later). The same technique was later used for a complex of fluorobenzene with fluoroform, and again, the agreement between the experimental blue shift and its theoretical prediction was good.[26]

The blue shift of the C−H stretch frequency was also theoretically predicted for C−H···O contacts. The first system investigated was fluoroform···oxirane,[27] where a significant blue shift of 30 cm^{-1} was predicted. The family of C−H···O complexes exhibiting a blue shift of the C−H stretch frequency upon complexation was later[28] extended to dimers of $F_nH_{3-n}CH$ with H_2O, CH_3OH, and H_2CO. These theoretical calculations predicted the largest blue shift of 47 cm^{-1} for the $F_3CH···OHCH_3$ complex. A very large blue shift of the C−H stretch frequency, more than 100 cm^{-1}, was detected recently from infrared spectra of $X^-···H_3CY$ ionic complexes (X = Cl, Y = Br; X,Y = I), which were also thoroughly investigated theoretically,[29] with excellent agreement with experimental values.

Theoretical study of the improper, blue-shifting intermolecular H-bond is difficult, and the most accurate techniques should be applied. First, consider the structure evaluation and particularly the influence of the basis set saturation effect. Routinely the structure of a complex is optimized by a gradient technique on the basis set superposition error (BSSE)-uncorrected potential-energy surface and the final stabilization energy determined for the calculated structure by a posteriori applying BSSE corrections, e.g., the function counterpoise (CP) procedure proposed by Boys and Bernardi.[30] (For more brief discussion of the BSSE free techniques, see ref 31). Such a treatment is incorrect because both the final stabilization energy and also the structure and other properties (e.g., vibration frequencies) of a complex are affected by the BSSE correction. It should be included in the structure and properties determination at least at the CP approximation. The first evidence that the geometry and vibrational frequencies determined at both levels differ comes from early 1990s,[32] and the structures of a few small complexes were optimized with inclusion of the BSSE by hand. Such treatment is, however, not applicable for large complexes containing dozens of degrees of freedom. Simon, Duran, and Dannenberg[33] recently offered a straightforward and elegant solution. Their method allows evaluation of the gradient and Hessian of a complex at any level of sophistication. The authors[33] applied the CP-corrected gradient optimization on three small H-bonded complexes and demonstrated that various properties obtained from CP-corrected and standard PES differ significantly. Similar results were obtained in our laboratory using our own code for other H-bonded systems.[34] The first evidence about the role of BSSE on vibrational frequencies comes from ref 32.

The other problem concerns the calculation of the vibration frequencies of a molecular complex. Usually these are evaluated at the harmonic approximation using the Wilson FG analysis on the basis of BSSE-uncorrected Hessians. Vibrational frequencies are considerably anharmonic,[35] and moreover, CP corrections affect[33,36] their values. Both the uncorrected BSSE and harmonic approximation effects are serious because rather small values of blue shifts (between 10 and 100 cm^{-1}) are determined as a difference of rather large values (more than 3000 cm^{-1}). In the following sections we will show the importance of CP corrections for the evaluation of harmonic vibration frequencies as well as the differences between harmonic and anharmonic frequencies for several improper, blue-shifting H-bond complexes.

The main goal of the present review is investigation of the improper, blue-shifting intermolecular H-bonds. It must be mentioned, however, that in

addition to intermolecular H-bonds, intramolecular H-bonds also exist, which are known to be important in structure formation. Characterization of the intramolecular H-bond is not easy since the unperturbed characteristics are missing for comparison. In the case of the intermolecular H-bond, we describe the formation of the H-bond comparing the bond characteristics (bond length, vibrational frequency, etc.) in the isolated systems and the H-bonded system, which is impossible for the intramolecular H-bonding. The intramolecular H-bond is mostly studied in the liquid phase using the NMR spin−spin X−H coupling constants, which are decisive for the bond formation. Normally the X−H coupling constants decrease[3] upon formation of the intramolecular H-bond, but in some cases an increase of the X−H coupling constants was detected.[37−40] This was found in the liquid phase in connection with the so-called proximity effect. The proximity of a X−H bond to an atom of the same system bearing lone electron pairs may yield either an increase or a decrease of the corresponding ^1J(XH) coupling constants. The proximity effect was studied by Contreras et al.,[41−43] who showed that an increase of the ^1J(XH) coupling constant is accompanied by a shortening of the X−H bond length while its decrease is connected with the X−H bond elongation. To elucidate the proximity effects, the authors also theoretically investigated[41,42] the following binary complexes (CH_4···FH, H_2O···HCN, CH_4···H_2O, and HCN···H_2O) and found that the observed trends in changes of the ^1J(XH) coupling constants are due to the effect of the electric field. Since the applied electric field causes the systematic C−H bond elongation (contrary to the ab initio calculations showing a shortening of the methane C−H bond length in the CH_4···H_2O complex), the authors concluded that the nature of the dominating interaction in the studied complexes must be different for each case. However, no specific explanation for the changes of the ^1J(XH) coupling constants was given. There is no clear correspondence between the NMR and IR properties of the H-bonds with shortened X−H bond. The NMR experiments were limited to the intramolecular interactions, and the role of the internal constrain is unknown. We, however, believe that both experiments describe the same physical phenomenon.

The contraction of the C−H bond upon formation of the intramolecular C−H···O contacts was predicted in creatine and sarcosine[44] from ab initio calculations. The Bader AIM analysis gives evidence about the formation of the C−H···O intramolecular H-bond.

II. C–H···π Improper, Blue-Shifting H-Bond

1. Benzene···Carbon–Hydrogen-Donor Complexes

The existence of the O−H···π H-bond in benzene···HOH and benzene···$HOCH_3$ complexes initiated speculations about the existence of the C−H···π H-bond. The formation of the C−H···π bond was supported by experimental[45] and theoretical[46] findings of an equilibrium structure of the benzene dimer where the T-shaped arrangement of aromatic rings

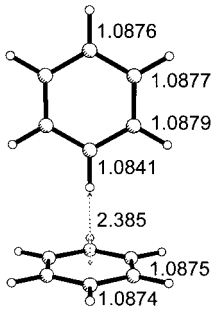

Figure 1. Structure and C−H bond lengths (in Å) of the T-shaped structure of the benzene dimer. The dashed line represents the distance between the center of one benzene ring and the closest hydrogen atom.

was believed to be stabilized by the adjoining C−H···π H-bond. The T-shaped arrangement of aromatic rings is rather common in a biological environment and stabilizes, e.g., the structure of phenylalanine.[47] This arrangement was also found in many crystal structures of molecules containing tetraphenylphosphonium cations.[48] Recently a dimer of tris(phenylthio)methane, having six equivalent T-shaped phenyl−phenyl interactions, was structurally determined. Quantum chemical calculations showed that this arrangement is quite stable.[49]

The benzene dimer was first investigated theoretically. The T-shaped structure of the dimer was optimized[24] at the correlated MP2/6-31G* level, and the resulting geometrical characteristics are shown in Figure 1. To our surprise, the C−H bond of the proton donor, which points to the center of the opposite benzene ring, is the shortest among all the C−H bonds. Improving the calculation did not change this result: extending the basis set to the 6-31G** level (i.e., adding p-polarization functions on hydrogens) gave exactly the same result. Harmonic vibrational frequencies were evaluated at both basis sets mentioned above, and contrary to expectation, the proton-donor C−H stretch vibration frequency did not predict the expected red shift typical for H-bonding but rather a large blue shift of 48 cm^{-1}. The C−H potential in the dimer is anharmonic, and therefore, there was doubt as to whether it is not the harmonic approximation that is responsible for the unexpected prediction of the blue shift. The anharmonic C−H stretch vibration frequency was estimated at three different levels. The simplest model, considering the one-dimensional C−H anharmonicity, provided an even larger blue shift (68 cm^{-1}) than the harmonic approximation. The two-dimensional model, which took into account the intermolecular benzene···benzene stretch in addition to the C−H stretch, provided a blue shift of 54 cm^{-1}. Finally, a model using effectively all of the remaining coordinates (for details see ref 24) predicted a blue shift of 56 cm^{-1}, similar to the two-dimensional approach. The anharmonic calculations confirmed the surprising results of the harmonic approximation, namely, the blue shift of the C−H stretch frequency of the proton donor upon dimer formation. The anharmonic calculations suggested that the harmonic treatment could be adequate; however, more experience is need.

A question arises whether formation of improper, blue-shifting H-bonds is limited only to the specific

Table 1. Characteristics of Benzene···Carbon Proton-Donor Complexes Evaluated at the MP2/6-31G* Level

complex[a]	q(H)[b]	ΔE[c]	Δr[d]	$\Delta\nu$[e]
$(C_6H_6)_2$	0.20	1.1	−0.0033	+49 (+42)
$C_6H_6\cdots HCN$	0.32	3.2	+0.0018	−16 (−18)
$C_6H_6\cdots HCCl_3$	0.30	3.2	−0.0025	+55 (+52)
$C_6H_6\cdots HCH_3$	0.17	0.3	−0.0008	+15 (+15)

[a] Cf. Figures 1 and 2. [b] Mulliken charge (in electrons) on isolated proton-donor hydrogen. [c] Stabilization energy (in kcal/mol) corrected a posteriori for the basis set superposition error. [d] Change of C−H bond length (in Å) of the proton donor upon formation of a complex; negative values mean shortening, while positive values mean elongation. [e] Change of the harmonic C−H stretch frequency (in cm^{-1}) of the proton donor upon formation of a complex; negative values indicate red shift, while positive values mean blue shift. Values in parentheses correspond to the MP2/6-31G** level.

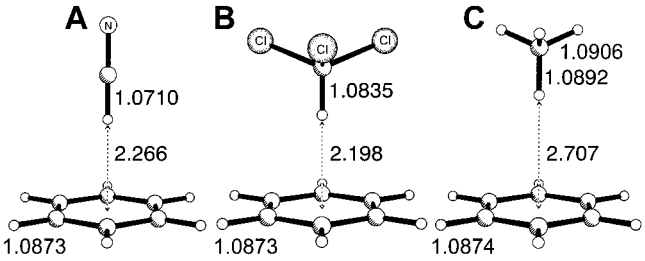

Figure 2. Structures of the benzene···X (X = HCN, CH_4, $CHCl_3$) complexes. All distances are in Å. The dashed lines represent the distance between the center of one benzene ring and the closest hydrogen atom.

case of the benzene dimer or whether it is a more general phenomenon and could be also observed in other carbon−proton-donor···benzene complexes. We studied the complexes of benzene with other carbon proton donors, HCN, CH_4, and $CHCl_3$. Characteristics of these complexes are presented in Table 1 and Figure 2. In the case of a strong proton donor like HCN, we found characteristic features of the classical H-bond, i.e., elongation of the C−H bond and the red shift of its stretch frequency. Although hydrogen atoms in $CHCl_3$ and HCN are of comparable acidity (see the hydrogen Mulliken charges in Table 1) and stabilization of the respective complexes with benzene is comparable, it is evident that the C−H bonds of these proton donors react differently to the complex formation (Table 1). While the bond is elongated in the case of HCN, it is contracted in $CHCl_3$. Similarly, the HCN C−H stretch frequency exhibits a red shift and the $CHCl_3$ C−H stretch frequency a blue shift. Even in the case of the benzene···methane complex, we found a small contraction of the C−H bond and a corresponding blue shift of its stretch frequency.

It is interesting that there is no correlation between the stabilization energy or C−H group hydrogen charge (from any population analysis) and the sign and value of the frequency shift.

2. Fluorobenzene···HCX_3 (X = F, Cl) Complexes

The title complexes were investigated both experimentally by infrared ion-depletion spectroscopy and theoretically by correlated ab initio methods.[25,26]

The first step in a theoretical study is a detailed investigation of the potential-energy surface (PES),

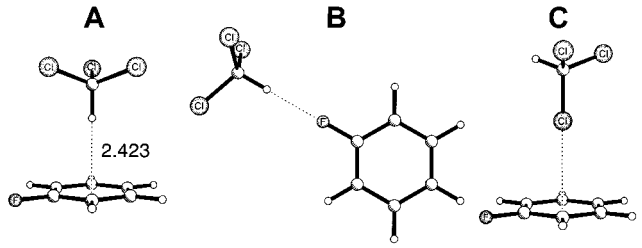

Figure 3. Structures of the fluorobenzene···chloroform complex (distance in Å).

Table 2. Characteristics of the Fluorobenzne···HCX_3 Complexes Determined at the MP2/6-31G* Level; Values in Parentheses Were Obtained at the MP2/6-31++G Level**

X	structure	optimization	ΔE[a]	Δr[b]	$\Delta\nu_h$[c]
Cl	sandwich[d]	standard	2.5	−0.003	67
		CP-corrected	3.1	−0.009	21
F	sandwich[e]	standard	1.6 (2.1)	−0.007 (−0.003)	38
		CP-corrected	2.2 (2.4)	−0.002 (−0.002)	31
	planar[e]	standard	1.4 (2.3)	−0.003 (−0.001)	-
		CP-corrected	1.7 (2.3)	−0.002 (0)	-

[a] Stabilization energy (in kcal/mol); in the case of standard optimization, it was a posteriori corrected for the BSSE. [b] Change of C−H bond length (in Å) of the HCX_3 upon formation of a complex. [c] Change of harmonic C−H stretch frequency (in cm^{-1}) of the HCX_3 upon formation of a complex. [d] Figure 3A. [e] Figure 4.

and care should be paid to the proper handling of the basis set superposition error. Besides the standard gradient optimization (which does not consider the BSSE), we have also used the CP-corrected gradient optimization. The latter optimization eliminates the BSSE in each gradient cycle, and hence, both inter- and intramolecular coordinates are corrected for the BSSE. Consider first a complex of fluorobenzene (Fb) with chloroform. Structures of the complex found by the standard gradient optimization at the MP2/6-31G* level are visualized in Figure 3. The structure with the C−H···π contact (Figure 3A) corresponds to a global minimum; the other structures with C−H··· F and C−Cl···π contacts are less stable. It should be mentioned that the starting geometry for the structure shown in Figure 3C was an umbrella-like arrangement with all three chlorine atoms directed symmetrically toward the π-cloud of Fb. The characteristics of the global minimum, determined by both standard and CP-corrected gradient optimization procedures, are presented in Table 2. The C−H bond of the proton donor is contracted in the complex by 0.009 Å; the standard optimization also predicts a contraction of the C−H bond but its value is smaller. The harmonic vibrational analysis, using the CP-corrected geometry and CP-corrected Hessian, shows that the C−H stretch frequency of the $CHCl_3$ is blue-shifted in the complex by 21 cm^{-1}. Harmonic vibrational analysis on the BSSE-uncorrected PES (with BSSE-uncorrected geometry) gives a blue shift of 67 cm^{-1}. As mentioned in the case of benzene dimer, the C−H potential is, however, considerably anharmonic and anharmonicity should be properly considered. Contrary to the benzene dimer, both 1-D (C−H bond) and 2-D (C−H bond and intermolecular distance) potential-energy functions were corrected

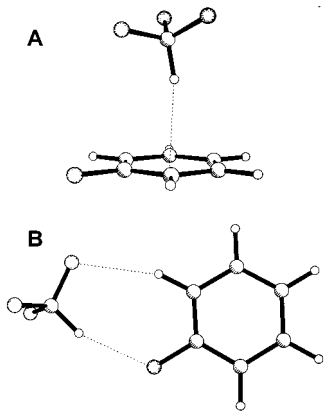

Figure 4. Sandwich and planar structures of the fluorobenzene···fluoroform complex with H···benzene center (A) and H···F (B) contacts. The filled circles represent fluorine atoms.

at each point for the BSSE (for details see ref 25). The 1-D anharmonic approximation corrected the blue shift to 16 cm^{-1}; the 2-D model decreases this value further to 12 cm^{-1}. The resulting calculated blue shift of the chloroform C−H stretch frequency agrees very well with the experimental value of 14 cm^{-1}. The experimental[25] blue shift of the C−H stretch frequency in benzene···$CHCl_3$ complex is very similar (15 cm^{-1}).

For the Fb···CHF_3 complex, two structures were considered, a sandwich (stacked) structure having a C−H···π contact and a planar structure with two C−H···F contacts (Figure 4). Structures found by standard and CP-corrected gradient optimizations are similar (Table 2). First, the BSSE-uncorrected results will be mentioned. While the 6-31G* calculations prefer the sandwich structure, extension of the basis set to 6-31++G** changes the order and the planar structure is slightly preferred by 0.2 kcal/mol. More reliable CP-corrected optimization prefers, with both basis sets, the sandwich structure to the planar one, by 0.5 kcal/mol at the MP2/6-31G* level. At the MP2/6-31++G** level, the stabilization energies are comparable for both structures. Unfortunately, the authors were not able to reduce the gradient norm for the sandwich structure at the CP-corrected MP2/6-31++G** optimization below 0.016 au. The stabilization energy, preferring the sandwich structure, should be thus larger than the calculated one. Nevertheless, the sandwich structure of the dimer is only slightly more stable then the planar one, which could result in coexistence of both isomers depending on the conditions. The coexistence of both isomers is supported by the value of energy barrier between both isomers of 2.5 kcal/mol, determined from standard MP2/6-31G* optimization.

The C−H bond of CHF_3 in the sandwich structure contracts upon complex formation. Optimizations with larger basis sets predict smaller contractions. The BSSE-uncorrected optimization technique predicts a larger contraction than the corrected one. The CP-corrected, MP2/6-31G*-calculated blue shift of the C−H bond vibration is 31 cm^{-1}, and the CP-uncorrected calculated value is 38 cm^{-1}.

While the standard optimization yields a larger shift for the sandwich structure of the Fb···$CHCl_3$ complex than the Fb···CHF_3 complex, the opposite is true for the CP-corrected optimization. The agreement of the blue shifts calculated using CP-corrected optimization with the experimental values (14 and 21 cm^{-1} for Fb···$CHCl_3$ and Fb···CHF_3, respectively) supports the use of this method.

Table 3. Characteristics of the Fluoroform···Ethylene Oxide Complex Determined at the MP2 Level with Various Basis Sets

basis set	structure[a]	optimization	ΔE^b	Δr^c	$\Delta\nu$
6-31G*	**A**	standard	3.0	−0.002	45
		CP-corrected	3.1	−0.002	37
	B	standard	2.5	−0.005	62
		CP-corrected	3.2	−0.003	50
6-31++G**	**A**	standard	3.8	−0.002	33
		CP-corrected	3.8	−0.001	27
	B	standard	3.9	−0.002	28
		CP-corrected	4.0	−0.003	39
6-31++G(2d,p)	**A**	standard	3.5	−0.001	29
		CP-corrected	3.5	−0.001	-
	B	standard	3.8	−0.003	43
		CP-corrected	3.9	−0.003	-

[a] Figure 5. [b] Stabilization energy (in kcal/mol); in the case of standard optimization, it was a posteriori corrected for the BSSE. [c] Change of C−H bond length (in Å) of the fluoroform upon complex formation. [d] Change of harmonic C−H stretch frequency (in cm^{-1}) of the fluoroform upon complex formation.

III. C–H···O Improper, Blue-Shifting H-Bond

C−H···O contacts in crystals of organic molecules has become topical in the past few years, and extensive literature is devoted to this subject.[2,3] It is believed that a weak H-bond is formed since the C···O distances are shorter than the sum of the van der Waals radii. The shortest C−H···O hydrogen bond was found in trinitromethane−dioxane−trinitromethane trimer.[50] The distance criterion is, however, not sufficient for formation of the H-bond because oxygen is a strong electron donor. The question arises whether all C−H···O interactions are classical H-bonds or whether the C−H···O improper, blue-shifting H-bonds also exist. To answer this question, we theoretically investigated several complexes with C−H···O contacts and found one candidate—the fluoroform···ethylene oxide (oxirane) complex.[27]

Five stationary points were found on the MP2/6-31G* CP-uncorrected potential-energy surface (Figure 5). Structures with C−H···O contacts (Figure 5A,B) are energetically more stable than these with C−H···F contacts (Figure 5C−E). Inclusion of BSSE corrections strongly affects both the absolute and relative stabilization energies, but the structures shown in part A and B of Figure 5 remain the most stable. Hence, only the C−H···O structures were investigated further. Table 3 contains characteristics of these two structures evaluated at the MP2 level with two different basis sets, 6-31G* and 6-31++G**. At the 6-31G* level, the CP-uncorrected stabilization energy prefers the "bent" structure shown in Figure 5B to the "linear" structure shown in Figure 5A. The a posteriori inclusion of the BSSE changes the order. However, the (CP-uncorrected) Hessian of the linear structure shown in Figure 5A possesses two negative eigenvalues and the structure thus does not cor-

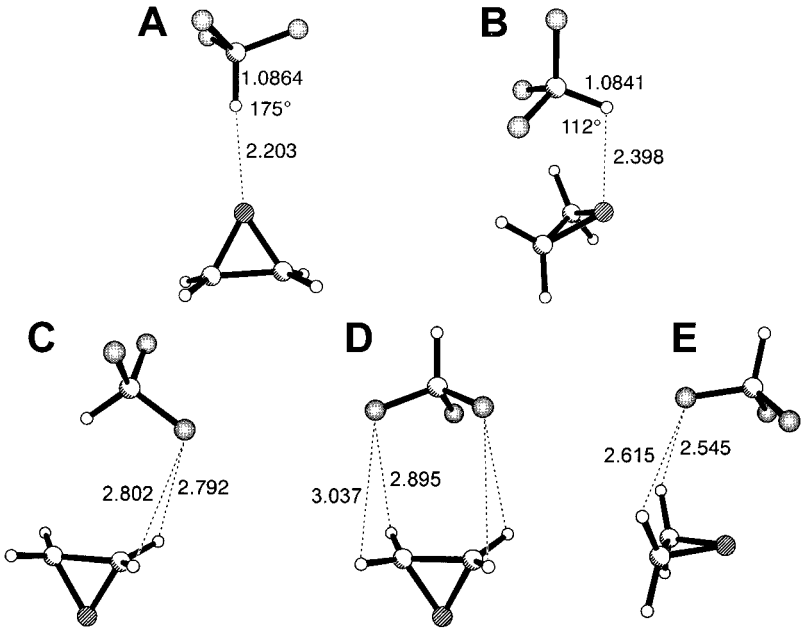

Figure 5. Structures of the ethylene oxide···fluoroform complex. The shaded circles represent oxygen atoms and the filled circles the fluorine atoms. The dashed lines correspond to the H···O and H···F contacts. Selected C−H bond lengths, interaction distances (in Å) and angles (in deg) are shown.

respond to a minimum. On the other hand, the bent structure shown in Figure 5B is a minimum; its Hessian has all positive eigenvalues. It is evident that inadequate use of the CP corrections, like the popular a posteriori technique, which corrects only energy at the stationary point of the uncorrected surface, can produce contradictory results. Performing all the calculations on a single PES does not have such shortcomings. The CP-corrected gradient optimization predicts a minimum for the bent structure shown in Figure 5B with all positive eigenvalues of the Hessian. With larger basis sets we obtain the correct relative energies already using the standard gradient optimization.

The linear structure shown in Figure 5A is less stable. The C−H bond is contracted, and the values of the contraction (and corresponding blue shift) are not very sensitive to the selection of the BSSE correction or the basis set. In the structure shown in Figure 5A, complex formation is accompanied by not only a blue shift of the C−H stretch frequency, but also with lowering of its intensity. This feature was not found for C−H···π improper, blue-shifting H-bond.

C−H···O interactions between the proton donor CF_nH_{4-n} (n = 1,2,3) and proton acceptor H_2O, CH_3OH, or H_2CO were investigated at various ab initio levels using various basis sets.[28] Characteristics of these complexes determined at the MP2/6-311+G** level are summarized in Table 4. The C−H bonds exhibit bond contraction and their stretch frequencies are blue shifted. The largest blue shifts were found for fluoroform complexes, with the fluoroform··· methanol complex being the greatest (Table 4).

The triformylmethane···chloroform structure, optimized at the MP2/SDD level[51] (i.e., valence double-ζ D95V basis set for the first-row atoms and Stuttgart/Dresden effective pseudopotentials for the Cl center),

Table 4. Stabilization Energy, ΔE (in kcal/mol), of $F_nH_{3-n}CH\cdots X$ Complexes (X = H_2O, CH_3OH, H_2CO), Change of C−H Bond Length, Δr (in Å), and Change of Harmonic C−H Stretch Frequency, $\Delta\nu$ (in cm^{-1}), of the Proton Donor upon Formation of a Complex (all values determined at the MP2/6-311+G level (taken from ref 28))**

	H_2O			CH_3OH			H_2CO		
	ΔE	Δr	$\Delta\nu$	ΔE	Δr	$\Delta\nu$	ΔE	Δr	$\Delta\nu$
F_3CH	2.3	−0.002	42	1.8	−0.002	47	2.6	−0.003	20
F_2HCH	2.7	−0.003	26	2.4	−0.002	20	2.5	−0.003	24
FH_2CH	1.7	−0.002	22	1.4	0.001	17	1.5	−0.002	19

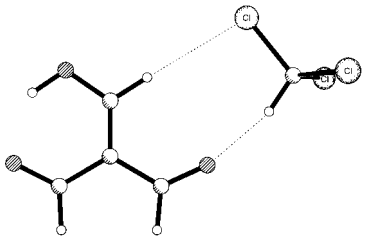

Figure 6. Planar dimer of triformylmethane with chloroform. The shaded circles represent oxygen atoms and the filled circles the chlorine atoms. This structure is the only minimum found on the PES.

is shown in Figure 6. The complex has a planar structure with C−H···O=C and C−H···Cl contacts. We have also tried to optimize a structure with the C−H···central triformylemethane carbon contact, but the optimization went to the same planar structure depicted in Figure. 6. The C−H bond of chloroform contracts by 0.002 Å upon formation of the complex while the C−Cl bond is elongated by 0.011 Å. The C−H stretch frequency of chloroform is blue shifted by 19 cm^{-1}. The experimental[21] blue shift of triformylmethane in liquid chlorofrom is 7 cm^{-1}.

Shortening of the C−H bond upon formation of the $CH_4\cdots OH_2$ complex was reported by Giribet et al. (ab initio HF/D95(d,p) level).[42]

Table 5. Interaction Energies (in kcal/mol) and Geometrical (in Å) and Vibrational (in cm^{-1}) Characteristics of $X^-\cdots H_3CY$ and $X^-\cdots HCH_3$ Complexes Evaluated at Standard and CP-Corrected MP2/SDD Levels (values in parentheses were obtained at the all-valence MP2/6-311G level)**

		ΔE	Δr(CH)	Δr(CY)	$\Delta\nu$(CH)[b] calcd	$\Delta\nu$(CY) calcd	$\Delta\nu$(CH)[b] exp
$Cl^-\cdots H_3CBr$[a]	standard	−9.96 (−8.54)	−0.0066 (−0.0040)	0.0702 (0.0354)	60, 89 (44, 57)	−141 (−76)	91, 119
	CP-corrected	−10.20	−0.0057	0.0567	53, 79		
$I^-\cdots H_3CI$[a]	standard	−5.53	−0.0039	0.0280	34, 50	−53	
	CP-corrected	−5.62	−0.0032	0.0246	31, 45	−45	
$Cl^-\cdots HCH_3$[a]	standard	−1.58	0.004		−51, −49		
$I^-\cdots HCH_3$[a]	standard	−0.56	0		−12, −18		−14, −20

[a] Cf. Figure 8. [b] Symmetrical and antisymmetrical vibrations.

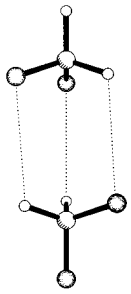

Figure 7. Global minimum of the difluoromethane dimer[52] with three H···F contacts.

IV. C–H···F Improper, Blue-Shifting H-Bond

The complex of difluoromethane (DFM) with water was investigated[52] experimentally using high-resolution absorption spectroscopy. Not only was the DFM··· water complex detected in the spectrum, but also other spectral lines were observed which were assigned to the formation of the $(DFM)_2$ dimer with C−H bonds of DFM acting as proton donors. The DFM molecule, having two hydrogen and two fluorine atoms, can act as a double proton donor and double proton acceptor. Consequently, the dimer can possesses multiple C−H···F contacts. The experimental rotation constants are consistent with the "double-umbrella" structure with three C−H···F contacts (Figure 7). The ab initio MP2/6-31+G** calculations confirmed[52] that this structure corresponds to a (hopefully global) minimum. Calculations have further shown[52] that upon complex formation the C−H bonds are contracted by 0.001, 0.001, and 0.002 Å and C−H stretch frequencies are blue shifted by 13, 13, and 20 cm^{-1}.

In connection with the study of the proximity effect, the $CH_4\cdots HF$ complex was investigated[41] at the MP2/D95**(d,p) level. It was found[41] that the C−H bond facing the F atom was slightly contracted.

V. C–H···X⁻ (X = Halogen) Improper, Blue-Shifting H-Bond

Very large blue shifts of the C−H stretch fundamentals were detected[29] in the anionic $X^-\cdots H_3CY$ (X = Cl, I; Y = Br, I) complexes by predissociation spectroscopy using a tandem time-of-flight photofragmentation spectrometer. Contrary to the halomethanes, methane (Y = H) displays a red shift upon complexation.

To describe the subsystems as well as the titled anion−molecule complexes consistently, the SDD

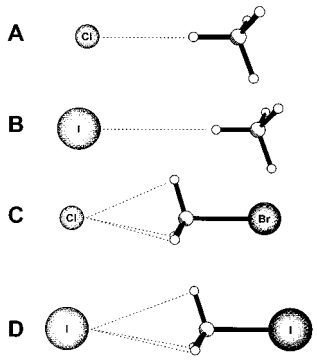

Figure 8. Structures of the $Cl^-\cdots H_3CBr$, $I^-\cdots H_3CI$, and $X^-\cdots HCH_3$ (X = Cl, I) anion−molecule complexes. Complexes **A** and **B** possess linear C−H···X^- classical hydrogen bonds, in contrast to the **C** and **D** trifurcated $(CH_3)\cdots X^-$ improper hydrogen-bonded complexes. The dashed lines correspond to the H···X^- contacts.

basis set, as implemented in the GAUSSIAN98 package,[51] was used, i.e., the valence double-ζ D95V basis set for the first-row atoms and the Stuttgart/Dresden effective pseudopotentials for the Cl, Br, and I centers. Note that relativistic effects are important for I, and therefore, all-electron calculations for iodine-containing systems, which neglect the relativistic effects, are not reliable. Figure 8 presents the calculated structures of the $Cl^-\cdots H_3CBr$ and $I^-\cdots H_3CI$ complexes, and the respective energy, geometry, and vibration characteristics are summarized in Table 5. Evidently these ionic complexes adopt structures with trifurcated $X^-\cdots H$ contacts (i.e., methyl "pocket" binding) with the methyl halides. The complexes with Cl^- are found to be more stable than the ones with I^-, and the calculated stabilization energy of the $Cl^-\cdots H_3CBr$ complex slightly decreased if an all-electron description is used. We found that the C−H bonds in the $X^-\cdots H_3CY$ complexes contract upon complex formation while C−Y bonds are elongated, and effects are most pronounced for the $Cl^-\cdots H_3CBr$ complex. Changes in bond lengths vary only slightly with different basis sets. Harmonic vibrational analysis revealed an increase in the C−H stretch frequency and a decrease in the C−Y stretch frequency upon complex formation. In all complexes investigated theoretically, the C−H blue shift is largest for $Cl^-\cdots H_3CBr$.

The situation changes when halogen is substituted for hydrogen, i.e., in anion−methane complexes. The global minima for both anion−methane complexes possess a linear $X^-\cdots HC$ arrangement (Figure 8). The formation of the complex is accompanied by elongation of the C−H bond engaged in the $X^-\cdots HC$ contact

(Table 5), with a concomitant red shift of the corresponding C−H stretch frequency. Although the elongation of the C−H bond in the $I^-\cdots HCH_3$ complex is rather small, the corresponding red shift is not negligible. Characteristics found for $X^-\cdots H_3CY$ complexes are thus typical for the improper, blue-shifting H-bonding, while those of $X^-\cdots HCH_3$ are typical for the standard H-bonding. The results for $Cl^-\cdots H_3CBr$ and $Cl^-\cdots HCH_3$ complexes were confirmed by all-electron calculations at MP2/aug-cc-pVDZ and MP2/aug-cc-pVTZ levels.

The highly symmetrical structure of the $Cl^-\cdots H_3CBr$ complex has the 3175 cm^{-1} band split into evenly spaced peaks[29] separated by about 10 cm^{-1}. Until now, this is the only experimental evidence that the complex adopts the C_{3v} symmetry. The main experimental observation is that the C−H stretch modes display very large blue shifts (more than 100 cm^{-1}), with a maximum for the $Cl^-\cdots H_3CBr$ complex. On the other hand, the C−H stretch vibrations in $X^-\cdots HCH_3$ complexes are red shifted upon complex formation and the absolute value of this shift is smaller than that in the case of former anion−molecule complexes. The good agreement between experimental and theoretical C−H stretch vibrational shifts is notable.

VI. Nature of H-Bonding and Improper, Blue-Shifting H-Bonding

1. Role of Dispersion Energy

What is the driving force for the formation of an improper, blue-shifting H-bond? In the case of classical H-bonding, the elongation of the X−H bond increases the dipole−dipole attraction between the proton donor and proton acceptor. In this type of H-bonding, the electrostatic interaction is the dominant stabilization energy contribution and also the CT term in not negligible.[3,53] In the case of benzene-containing complexes with an improper H-bond, the London dispersion energy is the dominant stabilization energy contribution and is proportional to the sixth power of the reciprocal distance between centers of mass of both subsystems. To maximize the attraction, the C−H bond of the proton donor is contracted. The molecule should "pay" for the contraction of the C−H bond, but the gain from the dispersion energy increase is larger. The theory successfully explains the relative value of the blue shifts for benzene···X (X = methane, benzene, and chloroform) complexes (cf. Table 1); the polarizabilities of methane, benzene, and chloroform increases, and hence, the London dispersion energies increase also. On the other hand, it fails to explain the relative values of the blue shift for fluorobenzene···X (X = fluoroform, chloroform) complexes. The polarizability of chloroform is larger than that of fluoroform, in agreement with the stabilization energy value (cf. Table 2), but the blue shift is larger for the fluorobenzene···fluoroform complex. It must be kept in mind, however, that in the case of dipolar systems, in addition to the dispersion energy, the induction term (dipole−induced dipole) also plays a role. This term is also proportional to the sixth power of the reciprocal distance. We believe that the dispersion term at least partly explains the nature of improper, blue-shifting H-bonding, but evidently additional terms are required for the correct explanation of the improper H-bonding.

2. "Atoms in Molecules" (AIM) Topological Analysis[54]

To gain insight into the nature of H-bonding and improper, blue-shifting H-bonding, we performed a comparative analysis of electron density topology in complexes with both types of bonding.[55] By means of AIM analysis, features such as bond critical points (bcp) and paths of maximum electron density are used to draw molecular graphs. X−H···Y H-bonding is manifested by a charge density at a path connecting atoms H and Y. Electron density topological properties were investigated in the benzene complexes with CH_4, $CHCl_3$, C_6H_6 (improper, blue-shifting H-bond), and HCN (H-bond).

Popelier[18] proposed a set of criteria for the existence of H-bonding. We investigated[55] whether these criteria are also fulfilled for improper H-bonding. The first condition is the existence of a bcp between hydrogen of proton-donor bond and an acceptor with a characteristic value of the electron density and laplacian of the charge density. This condition is satisfied for all of the complexes studied. The electron density at this bcp varies between 0.004 (CH_4) and 0.011 au ($CHCl_3$); the value for HCN is 0.009 au. The typical range for H-bonding is between 0.002 and 0.034 au. The second condition concerns mutual penetration of the hydrogen of the proton-donor and -acceptor atoms. In all complexes this penetration is positive, which agrees with previous data for H-bonded systems. The third condition is the loss of charge and decrease of the atomic volume of the hydrogen atom from the proton donor. In all cases we found a charge transfer from the aromatic ring to the proton-donor molecule, which was lowest for CH_4 (0.004 e) and comparable for all remaining donors (∼0.025 e). Similarly, the hydrogen-atom volume decreased in all cases. The last condition concerns the energetic destabilization and decrease of the dipolar polarization of the hydrogen from the proton donor. Energetic destabilization is always positive, ranging from 0.0034 to 0.0104 au, which agrees with the destabilization characteristics for H-bonding. The variation in the decrease of the dipolar polarization agrees with other H-bonded systems. We conclude that the Popelier criteria are valid for both complexes exhibiting features of classical H-bonding and improper, blue-shifting H-bonding. It is thus evident that the specific features of both types of H-bonding cannot be explained solely on the basis of changes of intermolecular electron densities or changes of the electron densities of hydrogen from a proton-donor molecule but can be explained by redistribution of the electron density in the C−H bond. The change in the electron density at C−H bcp gives a measure of the variation in the strength of the bond. We found a reasonable correlation between this change and both the corresponding change of the C−H bond lengths ($r = 0.99$) and the

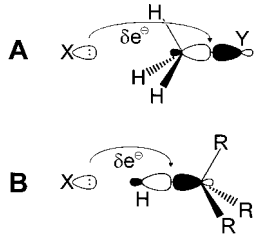

Figure 9. Schematic pictures of the electron density transfer (δe^-) in (A) improper, blue-shifting hydrogen-bonded complex and in (B) classical hydrogen-bonded complex. In the former case (A), the main electron density transfer goes from the electron lone pair of X to the C−Y σ^* antibonding orbital, while in the latter case (B), the electron density transfer goes to σ^* antibonding orbital of the C−H bond which is involved in the hydrogen bonding.

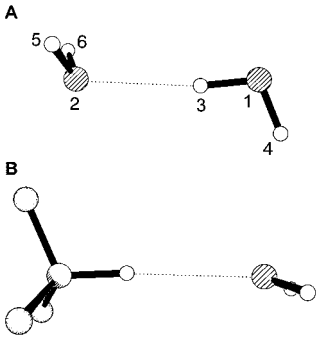

Figure 10. Schematic structures of the water dimer (A) and fluoroform···water (B) complex. The shaded circles represent oxygen atoms and the filled circles the fluorine atoms.

C−H stretch frequencies ($r = 0.94$). Similar results were obtained performing the AIM analysis for fluoroform···ethylene oxide complex.[56] To distinguish between H-bonding and improper H-bonding, it is necessary to extend the Popelier criteria with an additional condition concerning changes in the C−H bond upon complex formation. While classical H-bonding weakens this bond, the improper H-bonding strengthens it. Consequently, H-bonding exhibits a red shift of the X−H stretch frequency whereas the improper H-bonding exhibits a blue shift. The AIM analysis does not, however, reveal the origin of the bond strength changes in either type of H-bonding. This problem was solved by performing the natural bond orbital (NBO) analysis.

3. NBO Analysis of the Electronic Structure

Let us first repeat that the formation of a H-bonded complex involves charge transfer from the proton acceptor to the proton donor. Reed, Curtiss, and Weinhold[53] performed an NBO analysis for several typical H-bonded systems, demonstrating charge transfer from the lone pairs of the proton acceptors to the antibonding orbitals of the proton donor. For reference, we present the results of the NBO analysis for the benzene···water sandwich complex with a π···H−O H-bond, which is structurally similar to complexes investigated in this review. This analysis revealed the transfer of 4.8 me from benzene to water. The dominant part (4.2 me) of this transfer goes into the O−H antibonding orbital directed at the π-system of benzene. This increase of electron density in the OH antibonding orbital results in the OH bond elongation.

Let first examine the ion−molecule clusters with the largest blue shifts. The NBO analyses revealed[29] charge transfer from X^- to H_3CY (74 me in the case of $Cl^-\cdots H_3CBr$ and 28 me for $I^-\cdots H_3CI$). Unlike the standard H-bonding described above, the dominant charge acceptor is the C−Y antibonding orbital (Figure 9A), which results in C−Y bond elongation. This elongation leads to geometrical reorganization of the CH_3Y molecular framework, where the C−H bonds are contracted and the C−H stretch frequencies are blue shifted. The $Cl^-\cdots H_3CBr$ complex exhibits both the largest C−X bond elongation and the greatest C−H vibrational frequency blue shift. The situation is entirely different for the ion−methane complexes, which exhibit standard H-bonding (see above). As the methane does not contain a halogen, the charge transfer is directed to the C−H antibonding orbital, which is closest to the X^- lone electron pair (Figure 9B). This gives rise to weakening of this C−H bond and, consequently, to elongation of this C−H bond accompanied by a red shift of the respective C−H stretch frequency.

On the basis of these NBO analyses, we can conclude that H-bonding is a direct process where the primary effect is the charge transfer from the proton acceptor to the X−H antibonding orbitals of the proton donor. An increase of the electron density in this orbital leads to weakening of X−H bond accompanied by its elongation. The improper H-bonding represents, on the other hand, a more complicated "two-step" process. The charge transfer from the lone pairs of the electron donor is mainly directed to the antibonding orbitals in the remote part of the complex, which causes the elongation of bond(s) in that part of a complex. This primary effect is accompanied by a secondary effect of structural reorganization of the proton donor, leading to a contraction of the X−H bond and a blue shift of the X−H stretch frequency.

The origins of H-bonding and improper, blue-shifting H-bonding also differ in the water dimer and fluoroform···water complexes. Both complexes were theoretically studied by Gu and Scheiner,[28] who demonstrated that the first complex exhibits a red shift of the O−H stretch frequency while the second complex exhibits a blue shift of the C−H stretch frequency. The authors concluded[28] that this opposite pattern is not due to any fundamental distinction between the two interactions and that the C−H···O interactions in the $F_3CH\cdots OH_2$ complex can be categorized as a classical H-bonds. Let us first discuss the results of the NBO analysis for the H-bonded water dimer (Figure 10). The dominant part of the electron density transfer (EDT) originates from the oxygen $O_{(2)}$ lone pairs (10.2 me) and mainly goes (10.6 me) to the $O_{(1)}-H_{(3)}$ antibonding σ^* orbital. This increase in electron density weakens the $O_{(1)}-H_{(3)}$ bond, resulting in its elongation and a concomitant red shift of its O−H stretch frequency, in full agreement with what is known about the origin of the H-bond.[53] The situation with the fluoroform···water complex (Figure 10) is, however, different. There is not any EDT to the C−H antibonding σ^* orbital of

fluoroform. The EDT goes dominantly into the lone pairs of the fluorine atoms (3.3, 4.6, and 4.6 me). Besides the large electron flux mentioned above, we also detected a smaller decrease of electron density in all three C−F σ^* orbitals (−1.8, −1.0, −1.0 me) and the C−H antibonding σ^* orbital (−1.7 me). In addition to intermolecular EDT, the electron density of fluoroform undergoes an internal rearrangement. These principal changes in electron density account for 7.0 me of the total (7.1 me) EDT. What is the interpretation of the NBO results for the fluoroform···water complex? The dominant feature of the overall EDT is the increase of electron density at lone electron pairs of all fluorines in fluoroform. This is the primary effect which causes elongation of all C−F bonds. Elongation of the C−F bonds induces structural reorganization of the CHF_3 pattern including contraction of the C−H bond. The harmonic vibrational analysis for this deformed (isolated) fluoroform predicts a C−H stretch frequency of 3232 cm^{-1}, blue shifted by 10 cm^{-1} with respect to that frequency in optimized fluoroform. We conclude that the hydrogen binding in the fluoroform···water complex is markedly different from the water dimer: the hydrogen bond in the former complex is classical while the hydrogen bond in the latter is improper, blue-shifting.

4. Analysis of Molecular Orbitals

We can consider the complex molecular orbitals as a combination of the subsystem (fragment) orbitals. The interaction (mixing) of the occupied orbitals of one subsystem with the virtual orbitals of the other subsystem leads to the intersystem electron density transfer with the structural consequences discussed above. The situation is, however, clear only for the strong complexes, like the anion−molecule complexes (see section V). In the case of the $CH_3Br\cdots Cl^-$ improper hydrogen bond, there is strong fragment orbital mixing between the HOMO orbital of the Cl^- (one of the degenere p orbitals directed toward methylbromide along its C_3 axis) and the LUMO orbital of methylbromide (C−Br antibonding σ^* virtual orbital). These interacting fragment orbitals form the HOMO of the complex, in which the electron density on Cl^- decreases and the density on CH_3Br increases. The electron density transfer into the C−Br antibonding orbital results in the C−Br bond elongation, which, as discussed above, has consequences in structural reorganization of the subsystem and finally in the blue shift of the C−H stretch vibrations.

VII. Conclusion

Accurate ab initio calculations revealed a new type of intermolecular binding which resembles the standard hydrogen bonding. Because both the shift in C−H stretching frequency and the electronic nature of this new type of hydrogen bonding differ from the classical H-bonding, we propose the name "improper, blue-shifting hydrogen bond". Standard H-bonding of the type X−H···Y is characterized by weakening of the X−H bond which causes elongation of this bond and a red shift of the X−H stretch frequency. An improper, blue-shifting X−H···Y H-bond is, on the other hand, characterized by strengthening of the X−H bond which causes contraction of this bond and a blue shift of the X−H stretch frequency.

Blue shifts of the X−H stretch frequencies were experimentally found in the liquid phase (C−H···O type) as well as in the gas phase (C−H···X^-, C−H··· π types) and are smaller ($\sim$10 cm^{-1}) than those in a gas phase (10−100 cm^{-1}).

On the basis of various theoretical analyses ("atoms in molecule" topological analysis, natural bond orbital analysis, analysis of the shape of occupied MO), we have demonstrated the different origins of the standard H-bond and the improper, blue-shifting H-bond. Both types of H-bonds are characterized by electron density transfer from the proton acceptor (Y) to the proton donor (X−H). In the case of the standard H-bond, the dominant part of the electron density transfer from lone electron pairs or a region of π-electrons is directed to the X−H σ^* antibonding orbital of the proton acceptor. The increase of electron density in the σ^* orbital causes weakening of the X−H bond and its elongation and concomitant red shift of the X−H stretch frequency. The situation is basically different in the case of improper, blue-shifting H-bonding. First, there is no electron density transfer to the X−H σ^* antibonding orbital. The dominant part of the electron density transfer is directed to a remote part of the proton-donor molecule, mostly to C−Y σ^* antibonding orbitals or to lone electron pairs of atom(s) Y, which are not directly involved in the X−H···Y contacts. This primary effect is followed by a secondary effect, structural reorganization of the proton donor framework with contraction of the X−H bond directly involved in the X−H···Y contact and a concomitant blue shift of its stretch frequency. Formation of the standard H-bond is thus a direct process, and the weakening of the X−H bond is a direct consequence of EDT. Formation of the improper, blue-shifting H-bonding is, on the other hand, an indirect process where the strengthening of the X−H bond results from structural reorganization induced by EDT from the donor to a remote part of the acceptor.

The improper, blue-shifting concept is of a general nature and stabilizes not only intermolecular complexes but might also appear in intramolecular systems. See the discussion on the proximity effect.[37−43] We further expect that any interaction between an alkyl group and an aromatic ring in a molecule could lead to this type of bonding. Specifically, we have shown that improper, blue-shifting H-bonding is responsible for the preferential stability of the gauche form of *n*-alkylbenzene over the trans form.

VIII. Acknowledgments

We acknowledge with gratitude the contributions of our co-workers, as cited in the references. We are especially grateful to Professor Dr. Bernhard Brutschy who took our theoretical predictions seriously and made the first experimental detection of the blue shift in the gas phase. This work was supported by grants from the Grant Agency of the Academy of Sciences of the Czech Republic (A4040904)

and the Grant Agency of the Czech Republic (203/98/1166). The financial support by the Center for Complex Molecular Systems and Biomolecules, Czech Republic (Project LN00A032 of MSMT CR), is acknowledged. Extremely time-consuming calculations were performed at the Stuttgart High Performance Computer Center on the NEC SX4 supercomputer. The granted computer time and the kind help are gratefully acknowledged.

IX. References

(1) Jeffrey, G. A. *An Introduction to Hydrogen Bonding*; Oxford University Press: New York, 1997.
(2) Desiraju, G. R.; Steiner, T. *The Weak Hydrogen Bond*; Oxford University Press: Oxford, 1999.
(3) Scheiner, S. *Hydrogen Bonding*; Oxford University Press: New York, 1997.
(4) Pauling, L. *J. Am. Chem. Soc.* **1931**, *53*, 1367.
(5) Suzuki, S.; Green, P. G.; Bumgarner, R. E.; Dasgupta, S.; Goddard, W. A., III; Blake, G. A. *Science* **1992**, *257*, 942.
(6) Pribble, R. N.; Garret, A. W.; Haber, K.; Zwier, T. S. *J. Chem. Phys.* **1995**, *103*, 531.
(7) Djafari, S.; Lembach, G.; Barth, H.-D.; Brutschy, B. *Z. Phys. Chem.* **1996**, *195*, 253.
(8) Djafari, S.; Barth, H.-D.; Buchhold, K.; Brutschy, B. *J. Chem. Phys.* **1997**, *107*, 10573.
(9) Legon, A. C.; Wallwork, A. L.; Warner, H. E. *Chem. Phys. Lett.* **1992**, *191*, 97.
(10) Legon, A. C.; Roberts, B. P.; Wallwork, A. L. *Chem. Phys. Lett.* **1990**, *173*, 107.
(11) Steiner, T.; Desiraju, G. R. *Chem Commun*. **1998**, 891.
(12) Steiner, T.; Tamm, M.; Grzegorzewski, A.; Schulte, M.; Veldman, N.; Schreurs, A. M. M.; Kanters, J. A.; Kroon, J.; van der Maas, J. *J. Chem. Soc., Perkin Trans. 2* **1996**, 2441.
(13) Andrews, A. M.; Hillig, K. W., II.; Kuczkowski, R. L. *J. Chem. Phys.* **1992**, *96*, 1783.
(14) Steiner, T.; Starikov, E. B.; Amado, A. M.; Teixeira-Dias, J. J. C. *J. Chem. Soc., Perkin 2* **1995**, 1321.
(15) Block, P. A.; Marshall, M. D.; Pedersen, L. G.; Miller, R. E. *J. Chem. Phys.* **1992**, *96*, 7321.
(16) Sodupe, M.; Rios, R.; Branchadell, V.; Nicholas, T.; Oliva, A.; Danneneberg, J. J. *J. Am. Chem. Soc.* **1997**, *119*, 4232.
(17) Aakeröy, C. B.; Seddon, K. R. *Chem. Soc. Rev.* **1993**, 397.
(18) Kock, U.; Popelier, P. L. A. *J. Phys Chem.* **1995**, *99*, 9747. Popelier, P. L. A. *J. Phys. Chem. A* **1998**, *102*, 1873.
(19) Maes, G.; Smets, J.; Adamowicz, L.; McCarthy, W.; VanBael, M. K.; Houben, L.; Schoone, K. *J. Mol. Struct.* **1997**, *410−411*, 315.
(20) Smets, J.; McCarthy, W.; Maes, G.; Adamowicz, L. *J. Mol. Struct.* **1999**, *476*, 27.
(21) Buděšinský, M.; Fiedler, P.; Arnold, Z. *Synthesis* **1989**, 858.
(22) Keshavarz, K. M.; Cox, S. D.; Angus, R. O., Jr.; Wudl, F. *Synthesis* **1988**, 641.
(23) Boldeskul, I. E.; Tsymbal, I. F.; Ryltsev, E. V.; Latajka, Z.; Barnes, A. J. *J. Mol. Struct.* **1997**, *436*, 167.
(24) Hobza, P.; Špirko, V.; Selzle, H. L.; Schlag, E. W. *J. Phys. Chem. A* **1998**, *102*, 2501.
(25) Hobza, P.; Špirko, V.; Havlas, Z.; Buchhold, K.; Reimann, B.; Barth, H.-D.; Brutschy, B. *Chem. Phys. Lett.* **1999**, *299*, 180.
(26) Reimann, B.; Buchhold, K.; Vaupel, S.; Brutschy, B.; Havlas, Z.; Hobza, P. *J. Am. Chem. Soc.*, submitted for publication.
(27) Hobza, P.; Havlas, Z. *Chem. Phys. Lett.* **1999**, *303*, 447.
(28) Gu, Y.; Scheiner, S. *J. Am. Chem. Soc.* **1999**, *121*, 9411.
(29) Kelley, J. A.; Weber, J. M.; Robertson, W. H.; Lisle, K. M.; Johnsson, M. A.; Havlas, Z.; Hobza, P. *J. Am. Chem. Soc.*, submitted for publication.
(30) Boys, S. F.; Bernardi, F. *Mol. Phys.* **1970**, *19*, 553.
(31) Two procedures are free of the BSSE. The perturbation method for calculation of intermolecular interactions is, by definition, free of the BSSE but is useless for practical calculations where subsystem geometry is to be optimized. The variational chemical Hamiltonian approach developed by Mayer (Mayer, I. *Int. J. Quantum Chem.* **1983**, *23*, 341) is very promising since it eliminates the nonphysical terms of the Hamiltonian that are due to the BSSE. Unfortunately, derivations of an implementation of the chemical Hamiltonian gradient formulae at various theoretical levels (beyond Hartree−Fock) are not yet available. Much hope was given also to local MP treatments (Braneld, K.; Dasgupta, S.; Goddard, W. A., III. *J. Phys. Chem. B* **1997**, *101*, 4851) which claimed to be also BSSE free. Unfortunately, practical calculations performed in our laboratory have shown very limited use of the local MP methods for the calculations of molecular complexes. Until now, the only practically applicable approach for eliminating the BSSE is the use of the standard counterpoise procedure.
(32) Bouteiller, Y.; Behrouz, H. *J. Phys. Chem.* **1992**, *96*, 6033.
(33) Simon, S.; Duran, M.; Dannenberg, J. J. *J. Chem. Phys.* **1996**, *105*, 11024.
(34) Hobza, P.; Havlas, Z. *Theor. Chem. Acc.* **1998**, *99*, 372.
(35) Buenker, P. R.; Jensen, P. *Molecular Symmetry and Spectroscopy;* NRC Researcch Press: Ottawa, 1998.
(36) Hobza, P.; Bludský, O.; Suhai, S. *Phys. Chem. Chem. Phys.* **1999**, *1*, 2073.
(37) Afonin, A. V.; Andriyankov, M. A. *Zh. Org. Khim.* **1988**, *24*, 1034.
(38) Satonaka, H.; Abe, K.; Hirota, M. *Bull. Chem. Soc. Jpn.* **1987**, *60*, 953; **1988**, *61*, 2031.
(39) Tufró, M. F.; Contréras, R. H.; Facelli, J. C. *J. Mol. Struct. (THEOCHEM)* **1992**, *254*, 271.
(40) Angelotti, T.; Krisko, M.; O'Connor, T.; Serianni, A. S. *J. Am. Chem. Soc.* **1987**, *109*, 4464.
(41) Vizioli, C.; Ruiz de Azúa, M. C.; Giribet, C. G.; Contréras, R. H.; Turi, L.; Dannenberg, J. J.; Rae, J. D.; Weigold, J. A.; Malagoli, M.; Zanosi, R.; Lazzeratti, P.; Weigold, J. A.; Malagoli, M.; Zanosi, R.; Lazzaretti, P. *J. Phys. Chem.* **1994**, *98*, 8585.
(42) Giribet, C. G.; Vizioli, C. V.; Ruiz de Azúa, M. C.; Contréras, R. H.; Dannenberg, J. J.; Masunov, A. *J. Chem. Soc., Faraday Trans.* **1996**, *92*, 3029.
(43) Contréras, R. H.; Peralta, J. E.; Giribet, C. G.; Ruiz de Azúa, M. C.; Facelli, J. C. *Annu. Rep. NMR Spectrosc.* **2000**, *41*, 55.
(44) Popelier, P. L. A.; Bader, R. F. W. *Chem. Phys. Lett.* **1992**, *189*, 542.
(45) Janda, K. C.; Hemminger, J. C.; Winn, J. S.; Novick, S. E.; Harris, S. J.; Klemperer, W. *J. Chem. Phys.* **1975**, *63*, 1419.
(46) Hobza, P.; Selzle, H. L.; Schlag, E. W. *Chem. Rev.* **1994**, *94*, 1767.
(47) Hunter, C. A.; Singh, J.; Thornton, J. M. *J. Mol. Biol.* **1991**, *218*, 837.
(48) Dance, I.; Scudder, M. *Chem. Eur. J.* **1996**, *5*, 481.
(49) Bock, H.; Havlas, Z.; Krenzel, V.; Sievert, M. *Angew. Chem.*, submitted for publication.
(50) Bock, H.; Dienelt, R.; Schoedel, H.; Havlas, Z. *J. Chem. Soc., Chem. Commun.* **1993**, 1792.
(51) Frisch, M. J.; Trucks, G. W.; Schlegel, H. B.; Scuseria, G. E.; Robb, M. A.; Cheeseman, J. R.; Zakrzewski, V. G.; Montgomery, J. A., Jr.; Stratmann, R. E.; Burant, J. C.; Dapprich, S.; Millam, J. M.; Daniels, A. D.; Kudin, K. N.; Strain, M. C.; Farkas, O.; Tomasi, J.; Barone, V.; Cossi, M.; Cammi, R.; Mennucci, B.; Pomelli, C.; Adamo, C.; Clifford, S.; Ochterski, J.; Petersson, G. A.; Ayala, P. Y.; Cui, Q.; Morokuma, K.; Malick, D. K.; Rabuck, A. D.; Raghavachari, K.; Foresman, J. B.; Cioslowski, J.; Ortiz, J. V.; Stefanov, B. B.; Liu, G.; Liashenko, A.; Piskorz, P.; Komaromi, I.; Gomperts, R.; Martin, R. L.; Fox, D. J.; Keith, T.; Al-Laham, M. A.; Peng, C. Y.; Nanayakkara, A.; Gonzalez, C.; Challacombe, M.; Gill, P. M. W.; Johnson, B. G.; Chen, W.; Wong, M. W.; Andres, J. L.; Head-Gordon, M.; Replogle, E. S.; Pople, J. A. *Gaussian 98*, revision A.7; Gaussian, Inc.: Pittsburgh, PA, 1999.
(52) Reed, A. E.; Curtiss, L. A.; Weinhold, F. *Chem. Rev.* **1988**, *88*, 899.
(53) Caminati, W.; Melandri, S.; Moreschini, P.; Favero, P. G. *Angew. Chem., Int. Ed. Engl.* **1999**, *38*, 2924.
(54) Bader, R. W. F. *Atoms in Molecules. A Quantum Theory*; Oxford University Press: Oxford, 1990.
(55) Cubero, E.; Orozco, M.; Hobza, P.; Luque, F. J. *J. Phys. Chem. A* **1999**, *103*, 6394.
(56) Cubero, E.; Orozco, M.; Luque, F. J. *Chem. Phys. Lett.* **1999**, *310*, 445.

CR990050Q